Energy Reports 8 (2022) 2448–2461

Contents lists available at ScienceDirect

Energy Reports

journal homepage: www.elsevier.com/locate/egyr

Research paper

Managing the harvested energy in wireless sensor networks: A priority Geo/Geo/1/k approach with threshold

Otim Patricia Angwech [a,*], Attahiru S. Alfa [a,b], B.T.J. Maharaj [a]

[a] Department of Electrical, Electronic and Computer Engineering, University of Pretoria, Lynnwood Rd, Hatfield, Pretoria, 0002, South Africa
[b] Department of Electrical and Computer Engineering, University of Manitoba, Winnipeg, Manitoba, Canada

ARTICLE INFO

Article history:
Received 4 December 2020
Received in revised form 26 May 2021
Accepted 19 January 2022
Available online xxxx

Keywords:
Wireless sensor networks
Energy harvesting
Leakage
Threshold

ABSTRACT

Wireless sensor networks face many challenges, the major one being energy. Batteries are the main source of energy for the sensor nodes. When the battery is depleted, it must either be charged or replaced. This may be expensive or impossible to do. Energy harvesting has been proposed as an alternative. The energy is harvested and then stored in a battery. However, even if the battery is not in use, it experiences current leakages. We study the performance of a single node, which has data packets and energy tokens. The energy that is harvested is kept in reserve as energy tokens in an energy buffer and utilised by the data packets for transmission. This paper investigates the impact of imposing a threshold on the token buffer of the system. The problem considered is managing the energy buffer by taking into account storage of energy, usage by the data packets and energy leakage. The proposed model considers the transmission of high and low priority data packets. To ensure that there are tokens available in the system to transmit the high-priority data packets in case the arrival rate of the low-priority data packets is too high at the expense of high priority data packets, a threshold is imposed on the token buffer. To illustrate our approach, a Geo/Geo/1/k system is modelled and finite Markov chain model tools are used to analyse it. Numerical examples, which show how performance measures such as the mean number of data packets and tokens in the system are affected by energy harvesting, leakage and threshold, are presented. From the results obtained we show that the model can be utilised in the analysis and control of a wireless sensor network, as it captures the usage and leakage of energy. A trade-off between threshold and rate of leakage exists.

1. Introduction

As a fundamental component of Internet of Things (IoT), Wireless Sensor Networks (WSNs) have drawn substantial interest in research (Patil and Fiems, 2018). Recent advances in technology have aided their growth in the last decade. WSNs are integral parts of various systems such as nuclear and chemical attack detection, home automation, healthcare, transportation systems, agriculture and environment (Akyildiz et al., 2002a). In the military, for example, self-organisation, rapid deployment and fault tolerance characteristics make WSNs suitable for military command, communications and control. To realise these applications and other sensor network applications, wireless and ad hoc networking techniques are required. Despite the numerous proposed algorithms and protocols for traditional wireless and ad hoc networks, these are not applicable to sensor networks for the following reasons (Akyildiz et al., 2002a,b):

- The nodes in sensor networks are massively deployed.
- The topology of sensor networks changes regularly.
- Sensor nodes are deployed in large numbers, which can be a couple of orders of magnitude higher than ad hoc nodes.
- The communication used by sensor nodes is mainly communication paradigm; on the contrary, ad hoc networks mainly use point-to-point communication.

WSN nodes may be deployed in orders of thousands, in events where dense deployment is required or close to this. The nodes are low-cost, have sensing, communication and data processing capabilities and are required to fit in modules that are usually the size of a match-box (Akyildiz et al., 2002a).

Besides size, there are other limitations on nodes in WSNs, such as extremely low consumption of power, the ability to adapt to the environment, being dispensable, having the ability to operate unattended and being inexpensive to produce (Akyildiz et al., 2002a). The lifespan of the sensors is heavily dependent on the power resources of the nodes, as the sensors are often inaccessible, making it difficult to change the power source. In addition, the size restriction of nodes makes power a scanty

* Corresponding author.
E-mail address: PatriciaAngwech@tuks.co.za (O.P. Angwech).

https://doi.org/10.1016/j.egyr.2022.01.159

resource in the sensor nodes. In some applications, small lithium cell batteries (usually 1 cm thick and 2.5 cm in diameter) are used and, to ensure that the operating life is long, the current drawn is less than 30 μA (Akyildiz et al., 2002a; Vardhan et al., 2000). These batteries can power the network for varying periods as they are typically influenced by the usage pattern of energy and level of activeness the nodes. In some applications, the batteries are either replaced or recharged during maintenance which may be costly. In other applications, such as IoT, battery replacement may not be an option (Mouapi et al., 2017). The failure of a few nodes whose batteries are drained is generally not a significant problem; however, it affects the overall performance of the WSN.

In Anastasi et al. (2009), the authors suggest that by controlling the communication subsystem, energy consumption is reduced. In a perfect situation, the communication subsystem should be off unless it is required and woken up when required. This idea is applicable in systems that are operational under dynamic power management and can be amalgamated into the medium access control. Despite developments and improvements in management of power, the restricted energy of the batteries endures as a constraint on long-living nodes in WSNs.

To extend the lifespan of the network and mitigate battery dependence, energy harvesting has been taken advantage of in WSNs (Sudevalayam and Kulkarni, 2010; Paradiso and Starner, 2005; Gunduz et al., 2014; Lu et al., 2014; Yang and Chin, 2016; Yang et al., 2017; Tadayon et al., 2013). Energy harvesting may be described as a process of generating energy from the ambient surroundings of a network in order to provide a constant power supply for nodes and the WSN altogether (Shaikh and Zeadally, 2016).

Energy harvesting models are vital in designing and evaluating energy harvesting systems. Depending on the arrival of energy, the models are divided into two major categories, namely stochastic and deterministic (Ku et al., 2016). Deterministic models are mostly used for applications in which the power intensity of the energy source is predictable or varies slowly and is dependent on an accurate forecast of the profile of the energy over an extended period. The major drawback of this model is that as prediction intervals are increased, modelling mismatch is encountered. In stochastic models, on the other hand, the process of energy renewal is assumed to be random. Information on the non-causal energy state is not required, therefore making it appropriate for applications with fluctuating energy states. However, modelling mismatch is encountered, as it is difficult to wholly comprehend the stochastic behaviour of the different energy sources. In addition to the two major models, there are other special models. In one of these models, the harvested energy is not from natural sources, but rather from RF signals. These signals are generated artificially by external devices (Mouapi et al., 2017) and are either random or deterministic. The quantity of energy harvested depends on two components, namely the channels from the transmitters to the harvesting receivers and the transmitted power of transmitters. These factors institute a trade-off between energy and the transfer of information in WSNs. In addition to harvesting models based on RF signals, hybrid models are also categorised as other special models. In these models energy harvesting is combined with conventional power supply. Bernoulli models, the exponential process and the Poisson process are a few of the stochastic models employed in energy harvesting (Ku et al., 2016; Kong et al., 2017).

The origin of queueing theory dates back to the context of telephone traffic in Erlang's work (Erlang, 1909). Since then, applications such as telecommunications and industrial engineering have fuelled the interest of queueing theory (Bhat, 2015). Queueing systems consist of customers (for example, packets, connections and systems) and servers that process the customers. A queueing model can be characterised by the arrival process of the customers, the service process, the number of servers in parallel and the queue capacity. Kendall's notation is used to represent a single node queue. The analysis of queueing systems can be done in either discrete or continuous time. While discrete-time models give the state of the system at discrete points in time, continuous-time models allow for the state of the system to be obtained at any time instant. Queueing theory and its models are widely applied in telecommunications and data networks. It is not surprising that it has found applicability in WSNs.

In Bhat (2015), Giambene (2014), Bertsekas et al. (1992), Kleinrock (1975), Alfa (2010), the authors have done significant work with regard to queueing models in WSNs.

1.1. Related work

Many models have been presented for energy harvesting in WSNs. Some authors propose that the nodes have energy-neutral operation, whereby the nodes consume less energy than the energy harvested (Yang and Chin, 2016). In communications, Yang and Ulukus (2011) study the energy consumption of a communication system with an energy harvesting capability in a deterministic setting. It is assumed that data and energy arrivals are known. The authors in Tutuncuoglu and Yener (2012) also consider a deterministic setting in which the optimal transmission policies are identified for minimal transmission completion time and short-term throughput. Ozel and Ulukus (2010) consider an information-theoretic approach. The authors assume that energy in the battery can be used by the data packet without any loss and that in consecutive time intervals, the amount of energy accounts for a sequence of random variables that are independent. The authors furnish a geometric interpretation for the allocation of power.

The autonomous nature of sensors in determining which data to transmit and when to transmit have prompted some researchers to present the approach employing game theory for power control games in WSNs (Machado and Tekinay, 2008; Charilas and Panagopoulos, 2010; Afsar, 2015; Shi et al., 2012). Niyato et al. (2007), focus on a solar-powered node that employs the sleep-wakeup strategy by using a game of bargaining. In Haddad et al. (2012) the hawk and dove game with nodes capable of energy harvesting are studied. The nodes transmit data at either high or low power. However, because of the complexity and enormity of topologies, the modelling and analysis of WSNs using game theory could have a low probability of reaching the desired rate (Ali and Singh, 2017). As the WSNs increase in size, describing all the scenarios and outcomes becomes more difficult and may be impossible.

Some authors have concentrated on the system design with regard to the desired size of the data and energy buffers (Zhang et al., 2013). Others have concentrated on the self-sustainability of energy-harvesting WSNs taking into account the constant rate of energy consumption, stochastic energy arrivals and an infinite battery capacity (Guruacharya and Hossain, 2018).

In Zareei et al. (2017), the proposed Markov model is used to analyse the flow of energy of the nodes coupled by energy and data queues. An optimal battery size is then obtained for the node. In Michelusi et al. (2013), the authors propose a Markov model that characterises the degradation battery status. In this model, the energy harvested is only available for a specified amount of time, which is geometrically distributed. The authors in Valentini et al. (2015), also study battery degradation. They add ageing and performance measures as average cost functions to the model. In Jornet and Akyildiz (2012), the authors propose a model that captures the correlation between the energy consumption process and the energy-harvesting process.

In De Cuypere et al. (2018), the model of the sensor node is a two-dimensional Markov chain with queues for data and energy. In the study the following assumptions are made: uncertainty in data acquisition, energy harvesting and depletion. It is also assumed that the rate of arrival of data and energy follow a Poisson process.

In other studies, dissimilar categories of traffic in packet-based networks are integrated. The authors employ priority scheduling. The scheduling is categorised in two groups, namely pre-emptive and non-pre-emptive (Walraevens et al., 2011). In a non-pre-emptive system, the high-priority event is only given service once the service is completed. On the contrary, in a pre-emptive system, as soon as a high-priority event enters the system the service is interrupted. In some works, the high-priority buffer was infinite and the low-priority buffer was finite (Jolai et al., 2010). In others, the state-transition matrix for the model is developed using a two-dimensional Markov chain Ma et al. (2013). The authors in Gelenbe (2015) propose a model in which the energy needs of nodes are met by an amalgamation of energy harvesting and a connection to the mains as a back-up when the batteries are drained. They model the system as a finite Markov chain and show that if an energy packet is not adequate to transmit one data packet, the system is stable under some conditions. The authors also assume that the arrival of energy tokens and data packets follow a Poisson process. In addition, it is assumed that the rate at which energy is harvested is sluggish in contrast to the rate of data transmission.

Susu et al. (2008) present a framework for stochastic characterisation of nodes in energy harvesting in WSNs. Using the framework properties, namely expected downtime and the probability of achieving a specific operation time, the lifetime of the network is obtained. In Patil et al. (2018), the authors present a WSN capable of energy harvesting. The WSN is modelled as a discrete-time queueing model with data buffering and energy consumption. A deterministic threshold policy is employed to determine the mean value of information. The authors impose a threshold on the value of the information and show that the data transmission by the sensor node increases in selectivity with less energy.

While queueing models for WSNs with energy harvesting capability have been studied, a proportion of these models is inadequate to capture the energy drawing process precisely in WSNs (Zhang and Lau, 2015; Jeon and Ephremides, 2015; Ashraf et al., 2017; Dudin and Lee, 2016; Ku et al., 2015).

1.2. Contribution

In our previous work (Angwech et al., 2020) we developed three models of the system and considered mainly the analysis of the system. In this work, a control mechanism of the system is considered by including a threshold that will allow us to influence the queue performance measure to some extent. The emphasis therefore, is on control, given two classes of data and leakage of tokens. However, for completeness some information about the three models developed in our previous work is included when necessary.

The work presented here is a build-up of the priority model in Angwech et al. (2020). A three-dimensional Markov chain with priority, leakage and threshold imposed on the energy queue is proposed. The arrival and service processes are both geometric. The proposed model is a Geo/Geo/1/k system with k buffer spaces and one server. To ensure that there are tokens in the system for transmission of HP packets, a threshold is imposed on the energy buffer. Above the threshold both the LP packets and HP packets are transmitted. Below the specified threshold only the HP packets are transmitted.

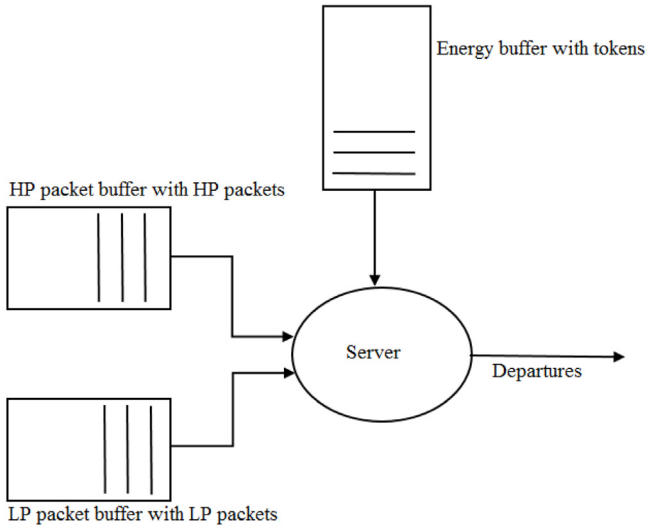

Fig. 1. System model.

To the authors' knowledge, a combination of priority and leakage of tokens with a threshold imposed on the token buffer has not been realised. The aim of this research is to capture the accumulation, dissipation and leakage of energy in the model.

2. System model

In this work, the proposed model is developed using a behavioural-box modelling technique. The model does not contain details on the framework of the electronic components but tries to imitate the input/output characteristics (Susu et al., 2008). The model of the server is a single-node queue in discrete time. This means that there is only one service location. Even if a packet finishes a service and re-enters immediately, it is still served by the exact servers in that location (Alfa, 2010).

A packet refers to one bit of data and a token refers to one bit of energy. The tokens and packets that can be queued are restricted; this implies that the buffers are finite. The assumptions below are made. In order to transmit a packet, a token is required. This indicates that on condition that a token is present in the token buffer, an arriving packet takes it out of the token buffer and uses it to enter the network. On the other hand, in the absence of tokens in the energy buffer, an arriving packet waits in its buffer. If the packet finds the data buffer full it is lost. Similarly, if an arriving token finds the energy buffer full, it is lost. Fig. 1 shows the proposed model.

The threshold is implemented as shown in Fig. 2 and is described as follows: Below a specified threshold, no LP packets are transmitted, while HP packets are continuously transmitted. The LP packets are only transmitted when the token buffer size is above the threshold. The assumption is that packets are transmitted before tokens leak.

3. Queueing analysis

3.1. Threshold model

In this work we study the impact of imposing a threshold on the priority model in Angwech et al. (2020).

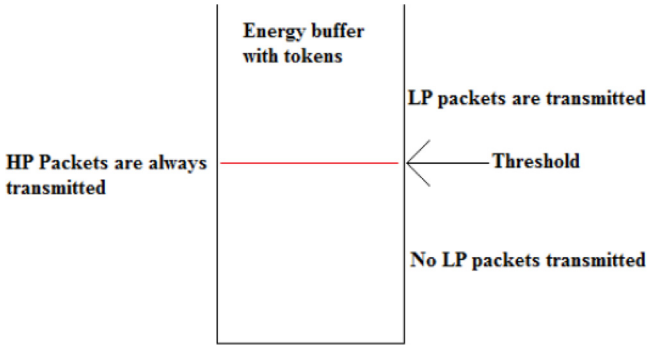

Fig. 2. System model with threshold incorporated.

3.1.1. Description

A system with two classes (low priority [LP] and high priority [HP]) of packets is considered. The arrival of packets is in line with the Bernoulli process, with a_L, the arrival rate of LP packets and a_H, the arrival rate of HP packets. Fig. 1 shows the proposed model. The threshold model has three buffers, one for the tokens, one for the LP packets and the other for HP packets. Like the priority model developed in Angwech et al. (2020), the threshold model is also a Geo/Geo/1 pre-emptive system. Taking into consideration system energy leakage, the following assumptions are made:

- A parameter θ (leakage probability) is introduced in the system. $1-\theta$ is the probability of no leakage.
- On arrival, a token remains in the system until the next transition (at least one unit), after which it leaks.
- Leakage occurs when there is at least one token in the system.

At time n in the system, when there are n tokens, the probability of having k tokens leak follows a binomial distribution given as:

$$l_{n,k} = \binom{n}{k}\theta^k(1-\theta)^{n-k}, n \geq k. \tag{1}$$

3.1.2. State space

A three-dimensional Markov chain is employed in the description of the state space of the model, (I_n, J_n, K_n), $n \geq 0$. At a time n, the following holds:

- I_n is the number of HP packets in the buffer $0 \leq I_n \leq M$
- J_n is the number of LP packets in the buffer $0 \leq J_n \leq N$
- K_n is the number of tokens in the buffer at $0 \leq K_n \leq K$

Where K is the buffer for the tokens, M is the buffer for the HP packets and N is the buffer for the LP packets. All the buffers are finite. A threshold is imposed on the token buffer, $0 \leq t \leq thresh$. At time n in the system, when there are t tokens, the probability of having k tokens leak is a binomial distribution given in Eq. (1), with $0 \leq n \leq t$

3.1.3. Transition matrix

Considering a state space of $\Delta = (i, j, k), i \geq 1, j \geq 1, k \geq 0$. The nature of the states of the Markov chain is studied using a state transition diagram from which a transition matrix is then obtained. For a threshold of three, the model was developed and state space obtained as shown in Tables 1–4. Imposing a threshold of three means that when there are fewer than three tokens, no LP packets are transmitted. For illustration purposes the tokens in the system are assumed to be four. CS is the current state.

Table 1
Threshold of three with a maximum of one token leaking.

(CS) 001	l_{10}	l_{11}
$a_{00}b$	002	001
$a_{00}\bar{b}$	001	000
$a_{01}b$	012	011
$a_{01}\bar{b}$	011	010
$a_{10}b$	102 (001)	101(000)
$a_{10}\bar{b}$	101(000)	100
$a_{11}b$	112 (011)	111(010)
$a_{11}\bar{b}$	111(010)	110

Table 2
Threshold of three with a maximum of two tokens leaking.

(CS)002	l_{20}	l_{21}	l_{22}
$a_{00}b$	003	002	001
$a_{00}\bar{b}$	002	001	000
$a_{01}b$	013 (002)	012	011
$a_{01}\bar{b}$	012	011	010
$a_{10}b$	103(002)	102 (001)	101(000)
$a_{10}\bar{b}$	102(001)	101(000)	100
$a_{11}b$	113(012)	112 (011)	111(010)
$a_{11}\bar{b}$	112(011)	111(010)	110

Table 3
Threshold of three with a maximum of three tokens leaking.

(CS)003	l_{30}	l_{31}	l_{32}	l_{33}
$a_{00}b$	004	003	002	001
$a_{00}\bar{b}$	003	002	001	000
$a_{01}b$	014 (003)	013 (002)	012	011
$a_{01}\bar{b}$	013 (002)	012	011	010
$a_{10}b$	104(003)	103(002)	102 (001)	101(000)
$a_{10}\bar{b}$	103(002)	102(001)	101(000)	100
$a_{11}b$	114(013)	113(012)	112 (011)	111(010)
$a_{11}\bar{b}$	113(012)	112(011)	111(010)	110

Table 4
Threshold of three with a maximum of four tokens leaking.

(CS)004	l_{40}	l_{41}	l_{42}	l_{43}	l_{44}
$a_{00}b$	005	004	003	002	001
$a_{00}\bar{b}$	003	003	002	001	000
$a_{01}b$	015(004)	014 (003)	013 (002)	012	011
$a_{01}\bar{b}$	014(003)	013 (002)	012	011	010
$a_{10}b$	105(004)	104(003)	103(002)	102 (001)	101(000)
$a_{10}\bar{b}$	104(003)	103(002)	102(001)	101(000)	100
$a_{11}b$	115(014)	114(013)	113(012)	112 (011)	111(010)
$a_{11}\bar{b}$	114(013)	113(012)	112(011)	111(010)	110

The transition matrix, P, is a classical QBD matrix and is given as follows:

$$P_{thresh} = \begin{bmatrix} B & C & & & \\ E & A_1 & A_0 & & \\ & A_2 & A_1 & A_0 & \\ & & \ddots & \ddots & \ddots \\ & & & A_2 & A_1 + A_0 \end{bmatrix}, \tag{2}$$

where

$$B = \begin{bmatrix} B_{00}^{00} & B_{01}^{00} & & & \\ B_{00} & B_{0,1} & B_{0,2} & & \\ & B_{0,0} & B_{0,1} & B_{0,2} & \\ & & \ddots & \ddots & \ddots \\ & & & B_{0,0} & B_{0,b} \end{bmatrix},$$

$$B_{00}^{00}=\begin{bmatrix} B_{000}^{000} & B_{001}^{000} & & & & \\ B_{000}^{001} & B_{001}^{001} & B_{002}^{001} & & & \\ B_{000}^{002} & B_{001}^{002} & B_{002}^{002} & B_{003}^{002} & & \\ \vdots & \vdots & \vdots & \vdots & \ddots & \\ B_{000}^{00K} & B_{001}^{00K} & B_{002}^{00K} & B_{003}^{00K} & \cdots & B_{00K}^{00K} \end{bmatrix},$$

with

$$B_{000}^{00n}=(a_{1,0}b+a_{0,0}\bar{b})l_{n,n}+a_{1,0}\bar{b}l_{n,n-1}$$

$$B_{001}^{00n}=a_{0,0}bl_{n,n}+(a_{1,0}n+a_{0,0}\bar{b})l_{n,n-1}+a_{1,0}\bar{b}l_{n,n-2}$$

$$B_{00t}^{00(t-1)}=a_{0,0}bl_{n,n-1}+(a_{1,0}n+a_{0,0}\bar{b}+a_{0,1}b)l_{n,n-2}+(a_{1,0}\bar{b}+a_{0,1}\bar{b})l_{n,n-3}$$

$$B_{00t}^{00(t)}=a_{0,0}bl_{n,n-2}+(a_{1,0}n+a_{0,0}\bar{b}+a_{0,1}b)l_{n,n-3}+(a_{1,0}\bar{b}+a_{0,1}\bar{b})l_{n,n-4}$$

$$B_{00K}^{00K}=a_{0,0}bl_{K,1}+(a_{1,0}n+a_{0,0}\bar{b}+a_{0,1}b)l_{K,0}+a_{0,0}bl_{K,0}$$

where

$$B_{01}^{00}=\begin{bmatrix} B_{010}^{000} & B_{011}^{000} & & & & \\ B_{010}^{001} & B_{011}^{001} & B_{012}^{001} & & & \\ B_{010}^{002} & B_{011}^{002} & B_{012}^{002} & B_{013}^{002} & & \\ \vdots & \vdots & \vdots & \vdots & \ddots & \\ B_{010}^{00K} & B_{011}^{00K} & B_{012}^{00K} & B_{013}^{00K} & \cdots & B_{01K}^{00K} \end{bmatrix},$$

with

$$B_{010}^{00n}=(a_{0,1}\bar{b}+a_{1,1}b)l_{n,n}+a_{1,1}\bar{b}l_{n,n-1},$$
$$B_{011}^{00n}=a_{0,1}bl_{n,n}+(a_{0,1}\bar{b}+a_{1,1}b)l_{n,n-1}+a_{1,1}\bar{b}l_{n,n-2}$$

$$B_{01K}^{00(K-1)}=a_{0,1}bl_{n,n-1}+(a_{0,1}\bar{b}+a_{1,1}b)l_{n,n-2}+a_{1,1}\bar{b}l_{n,n-3}$$

$$B_{01K}^{00K}=a_{1,1}bl_{K,t}+a_{1,1}bl_{K,(t-1)}+\cdots.+a_{1,1}bl_{K,(t-t)}$$

where

$$B_{00}=\begin{bmatrix} B_{010}^{000} & B_{010}^{001} & & & & \\ B_{011}^{000} & B_{011}^{001} & B_{011}^{002} & & & \\ B_{012}^{000} & B_{012}^{001} & B_{012}^{002} & B_{012}^{003} & & \\ \vdots & \vdots & \vdots & \vdots & \ddots & \\ B_{01t}^{000} & B_{01t}^{001} & B_{01t}^{002} & B_{01t}^{003} & \cdots & B_{01t}^{00K} \end{bmatrix},$$

with

$$B_{01(t-1)}^{00(t-1)}=a_{0,0}bl_{t-1,0},\quad B_{01t}^{00(t-1)}=a_{0,0}bl_{t,1}+a_{0,0}\bar{b}l_{t,0},$$
$$B_{01t}^{00t}=a_{0,0}bl_{t,0}$$

where

$$B_{0,0}=\begin{bmatrix} B_{020}^{010} & B_{020}^{011} & & & & \\ B_{021}^{010} & B_{021}^{011} & B_{021}^{012} & & & \\ B_{022}^{010} & B_{022}^{011} & B_{022}^{012} & B_{022}^{013} & & \\ \vdots & \vdots & \vdots & \vdots & \ddots & \\ B_{02t}^{010} & B_{02t}^{011} & B_{02t}^{012} & B_{02t}^{013} & \cdots & B_{02t}^{01t} \end{bmatrix},$$

with

$$B_{02(t-1)}^{00(t-1)}=a_{0,0}bl_{t-1,0},\quad B_{02t}^{00(t-1)}=a_{0,0}bl_{t,1}+a_{0,0}\bar{b}l_{t,0},$$
$$B_{02t}^{00t}=a_{0,0}bl_{t,0}$$

where

$$B_{0,1}=\begin{bmatrix} B_{010}^{010} & B_{011}^{010} & & & & \\ B_{010}^{011} & B_{011}^{011} & B_{012}^{011} & & & \\ B_{010}^{012} & B_{011}^{012} & B_{012}^{012} & B_{013}^{012} & & \\ \vdots & \vdots & \vdots & \vdots & \ddots & \\ B_{010}^{01t} & B_{011}^{01t} & B_{012}^{01t} & B_{013}^{01t} & \cdots & B_{01t}^{01t} \end{bmatrix},$$

with

$$B_{010}^{01t}=(a_{1,0}b+a_{0,0}\bar{b})l_{n,n}+a_{1,0}\bar{b}l_{n,n-1}$$

$$B_{011}^{01t}=a_{0,0}bl_{n,n}+(a_{1,0}b+a_{0,0}\bar{b})l_{n,n-1}+a_{1,0}\bar{b}l_{n,n-2},$$
$$B_{011t}^{01(t-1)}=a_{0,0}bl_{n,n-n}$$

$$B_{01t}^{01t}=a_{0,0}bl_{n,n-2}+(a_{1,0}b+a_{0,0}\bar{b})l_{n,n-n}+a_{0,0}bl_{n,n-n},$$
$$B_{01(K-1)}^{01K}=0,\quad B_{01K}^{01K}=(a_{1,0}b+a_{0,1}b)l_{K,0}$$

where

$$B_{0,2}=\begin{bmatrix} B_{020}^{020} & B_{021}^{010} & & & & \\ B_{020}^{021} & B_{021}^{011} & B_{022}^{011} & & & \\ B_{020}^{022} & B_{021}^{012} & B_{022}^{012} & B_{023}^{012} & & \\ \vdots & \vdots & \vdots & \vdots & \ddots & \\ B_{020}^{01t} & B_{021}^{01t} & B_{022}^{01t} & B_{023}^{01t} & \cdots & B_{02t}^{01t} \end{bmatrix},$$

with

$$B_{020}^{01t}=(a_{1,0}\bar{b}+a_{1,1}b)l_{n,n}+a_{1,1}\bar{b}l_{n,n-1},$$
$$B_{021}^{01t}=a_{0,1}bl_{n,n}+(a_{1,0}\bar{b}+a_{1,1}b)l_{n,n-1}+a_{1,1}\bar{b}l_{n,n-2}$$

$$B_{02t}^{01(t-1)}=a_{0,1}bl_{n,n-n},\quad B_{02t}^{01t}=a_{0,1}bl_{n,n-2}+(a_{0,1}\bar{b}+a_{1,1}b)l_{n,n-n}+a_{0,1}bl_{n,n-n},$$

$$B_{02(t-1)}^{01t}=0,\quad B_{02t}^{01t}=a_{1,1}bl_{t,0}$$

where

$$B_{0,b}=\begin{bmatrix} B_{0N0}^{0N0} & B_{0N1}^{0N0} & & & & \\ B_{0N0}^{0N1} & B_{0N1}^{0N1} & B_{0N2}^{0N1} & & & \\ B_{0N0}^{0N2} & B_{0N1}^{0N2} & B_{0N2}^{0N2} & B_{0J3}^{0N2} & & \\ \vdots & \vdots & \vdots & \vdots & \ddots & \\ B_{0N0}^{0Nt} & B_{0N1}^{0Nt} & B_{0N2}^{0Nt} & B_{0N3}^{0Nt} & \cdots & B_{0Nt}^{0Nt} \end{bmatrix},$$

with

$$B_{0Nt}^{0N0}=(a_{1,0}b+a_{0,0}\bar{b}+a_{0,1}\bar{b}+a_{1,1}b)l_{n,n}+(a_{1,0}\bar{b}+a_{1,1}\bar{b})l_{n,n-1}$$

$$B_{0Nt}^{0N1}=(a_{0,0}b+a_{0,1}b)l_{n,n}+(a_{1,0}b+a_{0,0}\bar{b}+a_{0,1}\bar{b}+a_{1,1}b)l_{n,n-1}+(a_{1,0}\bar{b}+a_{1,1}\bar{b})l_{n,n-2}$$

$$B_{0Nt}^{0N(t-1)}=(a_{0,0}b+a_{0,1}b)l_{n,n-1}+(a_{1,0}b+a_{0,0}\bar{b}+a_{0,1}\bar{b}+a_{1,1}b)l_{n,n-2}+(a_{1,0}\bar{b}+a_{1,1}\bar{b})l_{n,n-3}$$

$$B_{0N(t-1)}^{0Nt}=0,\quad B_{0Nt}^{0Nt}=(a_{1,0}b+a_{0,0}b+a_{0,1}b)l_{t,0}$$

where

$$C=\begin{bmatrix} B_{100}^{000} & B_{110}^{000} & & & \\ B_{100}^{001} & B_{110}^{001} & & & \\ B_{100}^{002} & B_{110}^{002} & & & \\ \vdots & \vdots & & & \\ B_{100}^{00K} & B_{110}^{00K} & & & \\ & C_{1,1} & C_{1,2} & & \\ & & C_{1,1} & C_{1,2} & \\ & & & \ddots & \ddots \\ & & & & C_{0,b} \end{bmatrix},$$

with

$$B_{100}^{00n}=a_{1,0}\bar{b}l_{n,n},\quad B_{110}^{00n}=a_{1,1}\bar{b}l_{n,n}$$

where

$$C_{1,1}=\begin{bmatrix} B_{110}^{010} & B_{110}^{011} & B_{110}^{012} & \cdots & B_{110}^{01t} \end{bmatrix}^{\mathrm{T}},$$

$$C_{1,2} = \begin{bmatrix} B_{120}^{010} & B_{120}^{011} & B_{120}^{012} & \cdots & B_{120}^{01t} \end{bmatrix}^{\mathrm{T}},$$

with

$$B_{110}^{01t} = a_{1,0}\bar{b}I_{n,n} \quad B_{120}^{01t} = a_{1,1}\bar{b}I_{n,n}$$

where

$$C_{0,b} = \begin{bmatrix} B_{1N0}^{0N0} & B_{1N0}^{0N1} & B_{1N0}^{0N2} & \cdots & B_{1N0}^{0Nt} \end{bmatrix}^{\mathrm{T}},$$

with

$$B_{1N0}^{0Nt} = (a_{1,0}\bar{b} + a_{1,1}\bar{b})I_{n,n}$$

where

$$E = \begin{bmatrix} E^1 & E^0 & & & \\ & E^1 & E^0 & & \\ & & \ddots & \ddots & \\ & & & E^1 & E^0 \\ & & & & E^b \end{bmatrix},$$

$$A_1 = \begin{bmatrix} A_1^1 & A_1^0 & & & \\ & A_1^1 & A_1^0 & & \\ & & A_1^1 & A_1^0 & \\ & & & \ddots & \ddots \\ & & & & A_1^1 + A_1^0 \end{bmatrix},$$

with

$$E^1 = \begin{bmatrix} a_{0,0}b & \cdots & 0 \end{bmatrix}, \quad E^0 = \begin{bmatrix} a_{0,1}b & \cdots & 0 \end{bmatrix},$$
$$E^b = \begin{bmatrix} a_{0,0}b + a_{0,1}b & \cdots & 0 \end{bmatrix},$$

$$A_1^1 = a_{1,0}b + a_{0,0}\bar{b}, \quad A_1^0 = a_{1,1}b + a_{0,1}\bar{b},$$

where

$$A_0 = \begin{bmatrix} A_0^1 & A_0^0 & & & \\ & A_0^1 & A_0^0 & & \\ & & A_0^1 & A_0^0 & \\ & & & \ddots & \ddots \\ & & & & A_0^1 + A_0^0 \end{bmatrix},$$

$$A_2 = \begin{bmatrix} A_2^1 & A_2^0 & & & \\ & A_2^1 & A_2^0 & & \\ & & A_2^1 & A_2^0 & \\ & & & \ddots & \ddots \\ & & & & A_2^1 + A_2^0 \end{bmatrix},$$

with

$$A_0^1 = a_{1,0}\bar{b}, \quad A_0^0 = a_{1,1}\bar{b}, \quad A_2^1 = a_{0,0}b, \quad A_2^0 = a_{0,1}b.$$

3.1.4. Performance measures

For a stable system the output, x is obtained such that Eq. (3) is satisfied.

$$x = xP, \quad x\mathbf{1} = 1, \tag{3}$$

where

$$x = [x_{000}, x_{001}, x_{002}, ..x_{00K}, x_{010}, x_{011}, x_{012}, \ldots, x_{01t}, x_{020}, x_{021}, x_{022}, \ldots, x_{0Nt}, x_{100}, x_{110}, \ldots, x_{1N0}, x_{200}, x_{210}, \ldots, x_{2N0}, \ldots, x_{MN0}].$$

To obtain the performance measures Eq. (4) is used. The mean number of tokens ($E_t[x]$), HP packets ($E_{hp}[x]$) and LP packets ($E_{lp}[x]$) in the system are as follows.

$$E_t[x] = \sum_{k=0}^{K} j x_{0,0,k} \qquad E_{lp}[x] = \sum_{j=1}^{N} i x_{0,j,0} \qquad E_{hp}[x] = \sum_{i=1}^{M} i x_{i,0,0} \tag{4}$$

4. Numerical examples

Having developed the models and established the Markov chain-based algorithms, we now assess the performance of the node. Further results with increased data points from the models obtained in Angwech et al. (2020) are presented in sections A, B and C.

Simulations are carried out and results are obtained with the following variables: the packet arrival rate (a), the token arrival rate (b), the buffer for the packets (F) and the buffer for the tokens (K).

For the priority and threshold models, the following variables are employed: the HP packet arrival rate (a_H), the LP packet arrival rate (a_L), the token arrival rate (b), the buffer for the HP packets (M), the buffer for the LP packets (N) and the buffer for the tokens (K).

For the threshold model, the parameters used in the priority model and a threshold imposed on the token buffer are used.

4.1. Basic model

In Fig. 3, we evaluate the impact of the data packet arrival rate on the mean number of tokens and packets in the system. As expected, an increase in the arrival rate of data packets results in an increase in the mean number of packets and a decrease in the mean number of tokens in the system.

4.2. Basic model with leakage incorporated

In Fig. 4, the effect of the data packet arrival rate on the mean number of tokens and packets in the system for the model, including leakage, is investigated. As expected, an increase in the rate of leakage results in a decrease in the mean number of tokens in the system.

Fig. 5 shows the probability of the HP packet buffer being full as the rate of leakage is varied. The probability of the HP packet buffer being full increases as the rate of leakage of tokens increases.

4.3. Priority model with leakage

In Fig. 6, the effect of the HP packet arrival on the mean number of tokens, LP packets and HP packets in the system for the model including leakage and priority is investigated. The results are as anticipated, with the mean number of HP packets increasing as the arrival rate of HP packets increases. The LP and HP buffers are both at full capacity when the arrival rate of HP packets is 1. This is because the arrival rate of tokens is kept constant.

In Fig. 7, the impact of the arrival rate of the energy tokens on the mean number of tokens, LP packets and HP packets in the system for the model including leakage and priority is investigated. In Fig. 8 we show the impact of varying the rate of the leakage on the mean number of tokens, LP packets and HP packets in the system. As expected, the results show that the mean number of packets (both HP and LP) increases with an increase in the rate of leakage. Leakage and usage by the HP and LP packets contribute to the decline in the mean number of tokens in the system.

4.4. Threshold model with leakage and priority

In Fig. 9 we investigate the impact of imposing a threshold and varying the HP packet arrival rate on the mean number of tokens and packets (both HP and LP) in the system. As we expect, the mean number of HP packets in the system increases with an increase in the arrival rate of HP packets.

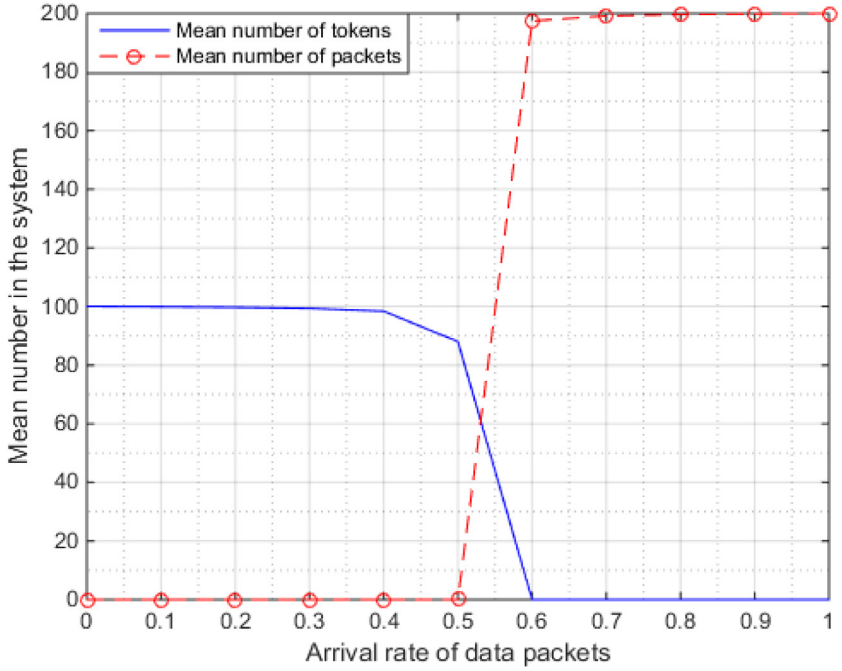

Fig. 3. The mean number of packets and tokens in the system as the data packet arrival rate is varied. Where a is varied, $b = 0.6$, $F = 200$ and $K = 100$.

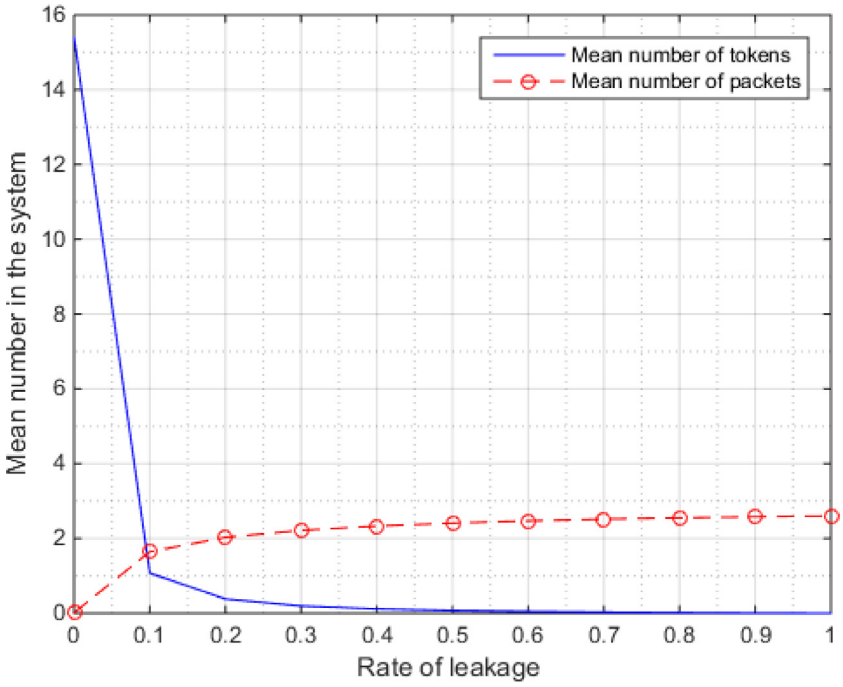

Fig. 4. The mean number of packets and tokens in the system as the rate of leakage of tokens is varied. Where θ is varied, $a = 0.52$, $b = 0.6$, $F = 72$ and $K = 18$.

In Fig. 10 we show the effect of imposing a threshold and varying the token arrival rate on the mean number of tokens and packets (both HP and LP) in the system.

In Fig. 11 we show the effect of imposing a threshold and varying the leakage rate on the mean number of tokens, LP packets and HP packets in the system. As expected, an increment in the rate of leakage results in a decrease in the mean number of tokens and an increment in the mean number of packets (both HP and LP). The decrease in the mean number of tokens in the system is attributed to a combination of usage by the packets and leakage.

In Fig. 12 the effect of increasing the rate of leakage from 0.01 to 0.15 is shown. In Fig. 13 the effect of decreasing the threshold is shown.

In Table 5, a_H is varied, $a_L = 0.2$, $b = 0.6$, $\theta = 0.05$, $M = 100$, $N = 40$, $K = 48$, $threshold = 5$, $threshold = 10$ and $threshold = 15$. It is observed that an increase in the threshold results in an increase in the mean number of LP packets in the system. Since the HP packets are always transmitted, the effect of the threshold on the mean number of HP packets is hardly noticeable.

In Table 6, the threshold is varied, $a_L = 0.2$, $a_H = 0.4$, $b = 0.4$, $\theta = 0.01$, $M = 100$, $N = 40$, $K = 48$. In Table 7, the threshold is

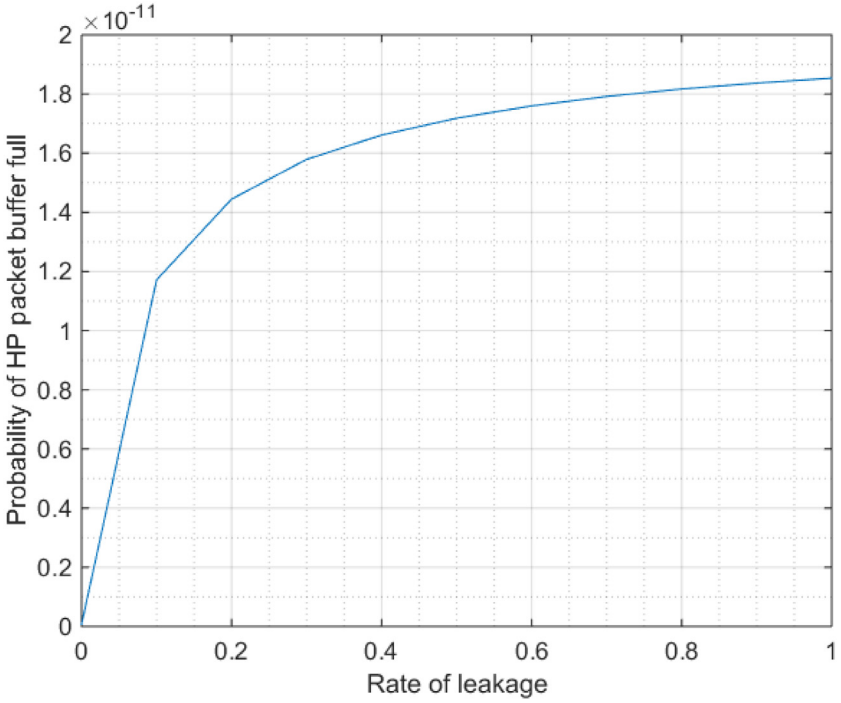

Fig. 5. Probability of the packet buffer full as the rate of leakage is varied. Where θ is varied, $a = 0.52$ $b = 0.6$, $F = 72$ and $K = 18$.

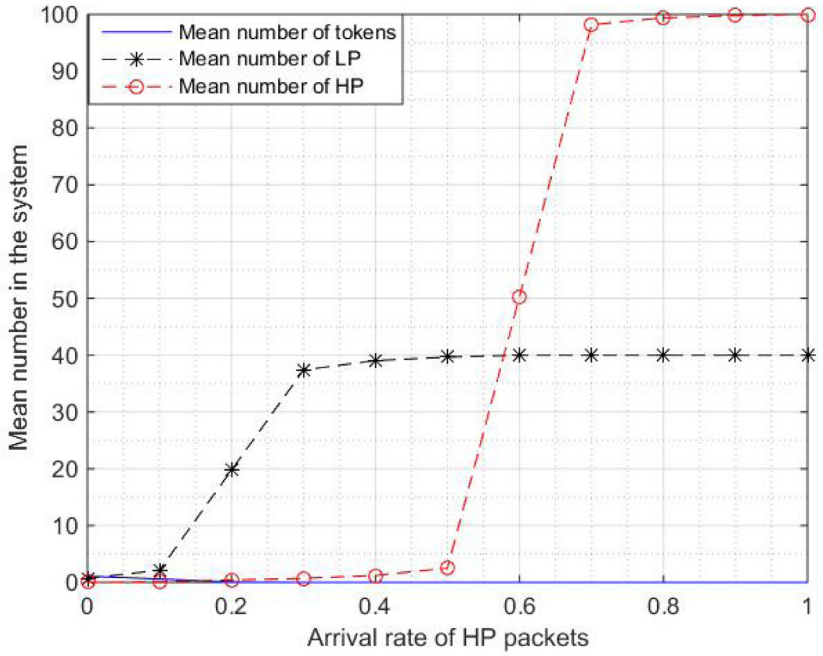

Fig. 6. The mean number of HP packets, LP packets and tokens in the system as the HP packet arrival rate is varied. Where a_H is varied, $a_L = 0.4$, $b = 0.6$, $\theta = 0.4$, $M = 100$, $N = 40$ and $K = 48$.

varied, $a_L = 0.6$, $a_H = 0.4$, $b = 0.4$, $\theta = 0.01$, $M = 100$, $N = 40$, $K = 48$.

5. Discussion

The results of the basic system modelled with packets and tokens are given in Fig. 3. From the figure it is observed that the packet and token buffers cannot be at maximum capacity at the same instant. This is expected, as an increment in the arrival rate of data packets results in a reduction in the mean number of tokens and an increase in the mean number of packets in the system. This is because a token is vital in processing a packet, resulting in a decrease in the mean number of tokens in the system as the arrival rate of packets increases.

In a practical system, tokens that are not used by the data packets may leak. The graph presented in Fig. 4 captures this. As expected, an increment in the rate of leakage results in a reduction in the mean number of tokens in the system. When the probability of leakage is 0, there is no leakage in the system, implying that there are tokens to be used by the packets. However,

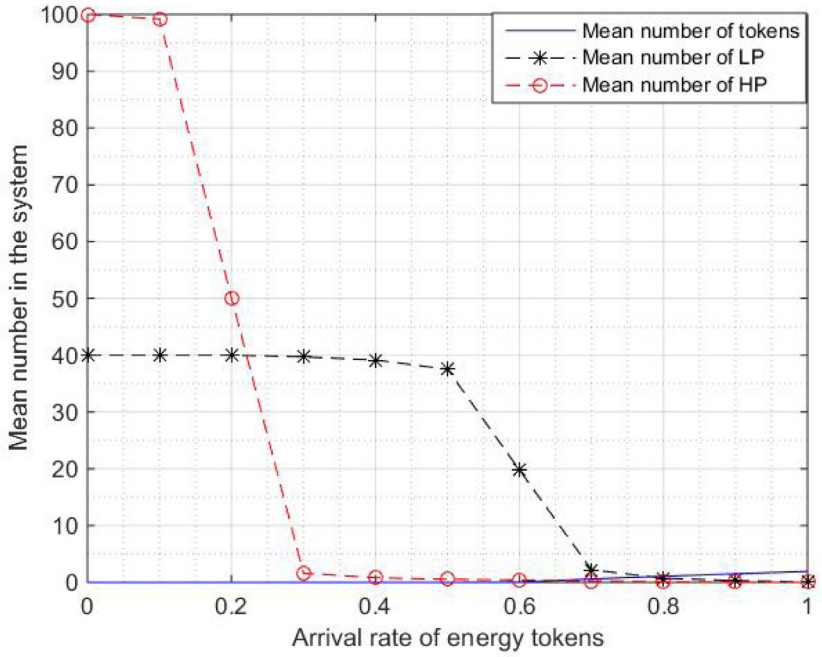

Fig. 7. The mean number of HP packets, LP packets and tokens in the system as the tokens arrival rate is varied. Where b is varied, $a_H = 0.2$, $a_L = 0.4$, $\theta = 0.4$, $M = 100$, $N = 40$ and $K = 48$.

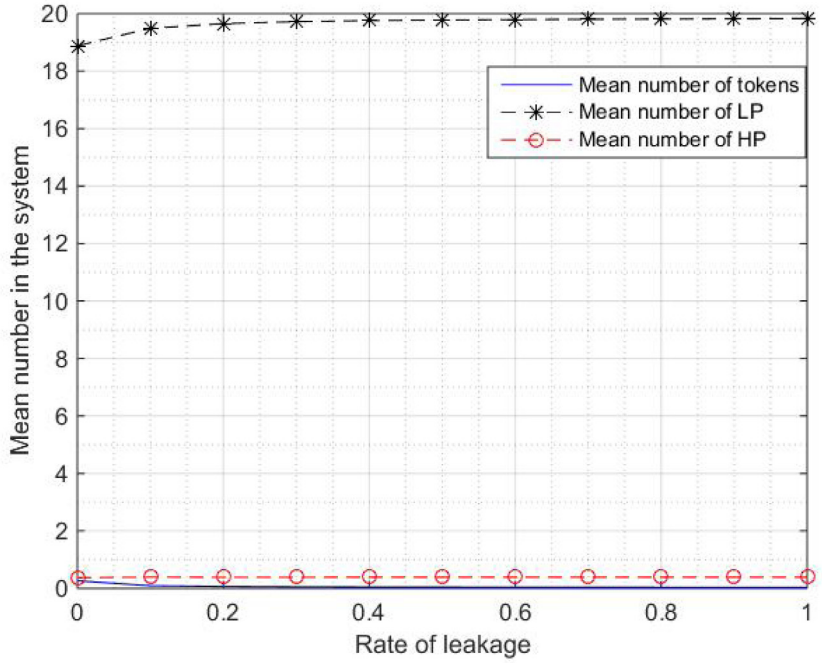

Fig. 8. The mean number of HP packets, LP packets and tokens in the system as the rate of leakage is varied. Where θ is varied, $a_H = 0.2$, $a_L = 0.4$, $b = 0.6$, $M = 50$, $N = 20$ and $K = 24$.

the token buffer is not full, as expected, as there are packets in the system (with an arrival rate, a, of 0.52) that use the tokens.

In addition to leakage, we also include emergency data (HP packets) which need to be transmitted immediately in the model. In this model both energy leakage and priority are included. The results are given in Fig. 6, 7 and 8. We observe that an increment in the arrival rate of HP packets results in a decrease in the mean number of tokens in the system and an increase in the mean number of LP and HP packets. The effect of the rate of leakage on the probability of the HP packet buffer being full is presented in Fig. 5.

In the priority model, we investigate the impact of leakage on the mean number of tokens, HP and LP packets in the system illustrated in Fig. 8. An increase in the rate of leakage results in a decrease in the mean number of tokens and an increase in the mean number of LP and HP packets. Finally, we demonstrate the consequence of imposing a threshold on the token buffer. This is illustrated in the threshold model whose results are shown in Fig. 9, 10 and 11.

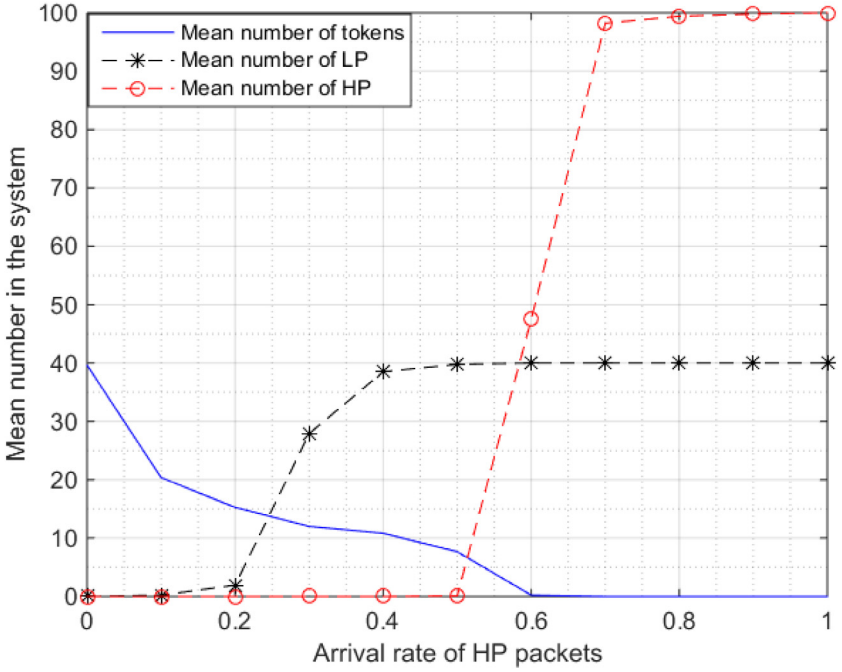

Fig. 9. The mean number of HP packets, LP packets and tokens in the system as the arrival rate of HP packets is varied. Where a_H is varied, $a_L = 0.2$, $b = 0.6$, $\theta = 0.01$, $M = 100$, $N = 40$, $K = 48$ and *threshold* $= 15$.

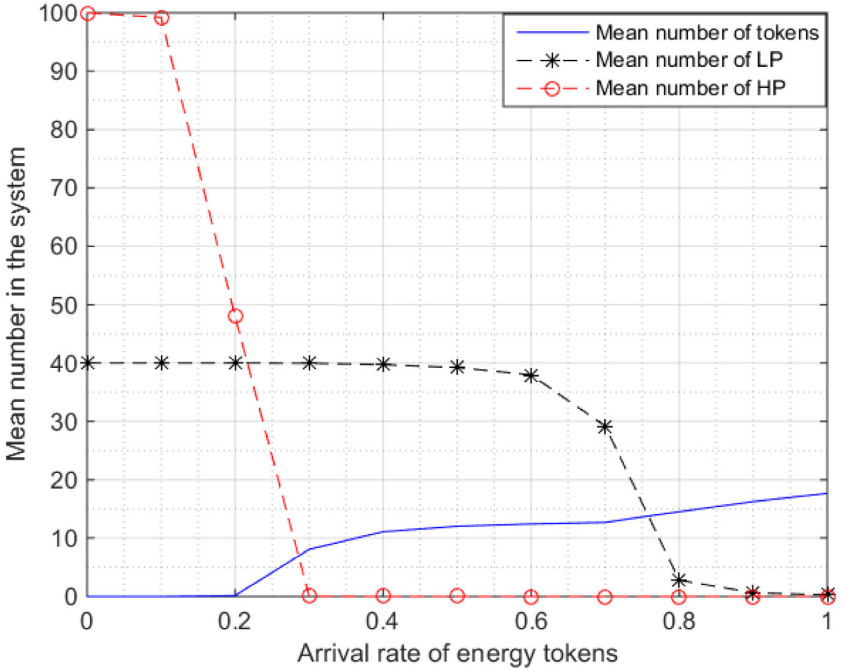

Fig. 10. The mean number of HP packets, LP packets and tokens in the system as the arrival rate of tokens is varied. Here b is varied, $a_H = 0.2$, $a_L = 0.4$, $\theta = 0.01$, $M = 100$, $N = 40$, $K = 48$ and *threshold* $= 15$.

We see that imposing a threshold on the token buffer results in a significant increment in the mean number of LP packets at lower arrival rates of HP packets in the system, as demonstrated in Fig. 9. An increment in the mean number of HP packets in the system results in an increment in the arrival rate of the HP packets. The probability of leakage, 0.15, is small, such that the effect of the threshold on the mean number of LP packets in the system is observed. A high probability of leakage results in fewer tokens in the system and therefore the LP packets will not be transmitted, as the threshold value will be reached faster.

In Fig. 11, we observe a sharp increase in the mean number of LP packets in the system when the rate of leakage increases from 0 to 0.1. The mean number of LP packets reaches the buffer size of the LP packet. This is expected, as the tokens available are used mainly by the HP packets. The threshold imposed ensures that the HP packets are constantly transmitted. The mean number of HP packets increases with an increase in the rate of leakage but never reaches full buffer size.

The effect of imposing a threshold on the token buffer is also shown in Figs. 12 and 13. The rate of leakage is increased to 0.15

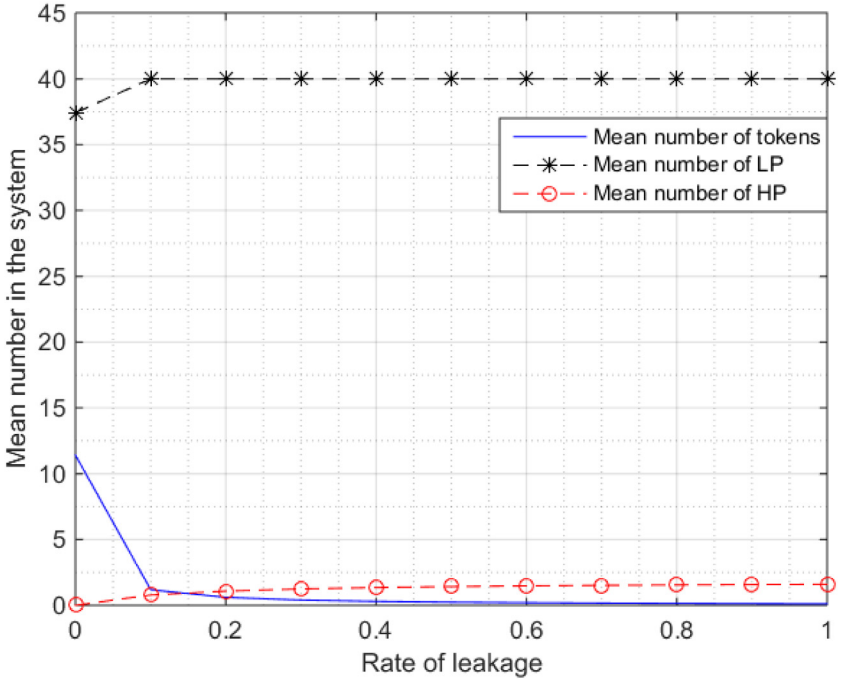

Fig. 11. The mean number of HP packets, LP packets and tokens in the system as the rate of leakage is varied. Here θ is varied, $a_H = 0.4$, $a_L = 0.2$, $b = 0.52$, $M = 100$, $N = 40$, $K = 48$ and *threshold* $= 15$.

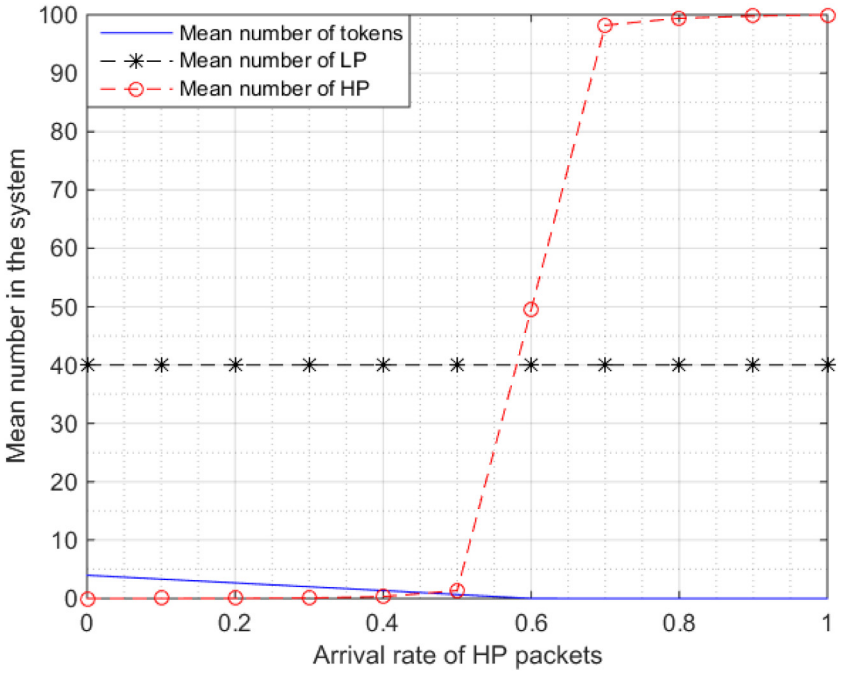

Fig. 12. The mean number of HP packets, LP packets and tokens in the system as the rate of leakage is varied. Here a_H is varied, $a_L = 0.2$, $b = 0.6$, $\theta = 0.15$ $M = 100$, $N = 40$, $K = 48$ and *threshold* $= 15$.

in both figures. In Fig. 12, the threshold is at 15, implying that more tokens either leak or are reserved for the HP packets in the system. Therefore, fewer LP packets will be transmitted, as shown in the figure. In Fig. 13, the threshold is reduced to 5. As expected, the mean number of LP packets is significantly affected.

In Table 5 the arrival rate of the HP packets is varied at three different thresholds while keeping the other parameters constant. When the threshold is at 5, the mean number of LP packets is lower than when the selected threshold is 10. This means that at a low threshold, there are more tokens available for transmission of LP packets in the system than when the threshold is at 10 or 15. An increase in the threshold implies that fewer tokens will be available in the system for the transmission of LP packets. This contributes to the increase in the mean number of LP packets in the system when the threshold is increased.

The results presented in Tables 6 and 7 show the effect of changing the arrival rate of tokens and LP packets in the system. The model presented is a pre-emptive queueing system, therefore increasing the arrival rate of LP packets has a very small impact on the mean number of HP packets in the system. The mean

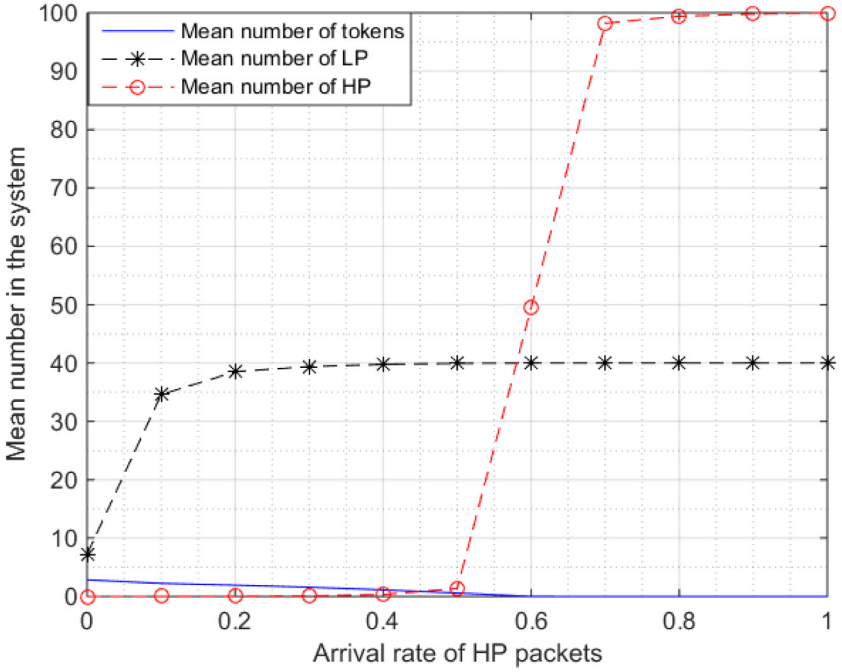

Fig. 13. The mean number of HP packets, LP packets and tokens in the system as the rate of leakage is varied. Here a_H is varied, $a_L = 0.2$, $b = 0.6$, $\theta = 0.15$ $M = 100$, $N = 40$, $K = 48$ and *threshold* $= 5$.

Table 5
Comparison of results obtained from the basic model with leakage, priority and threshold incorporated when the arrival rate of hp packets in the system is varied.

Arrival rate of HP packets	*Threshold* = 5		*Threshold* = 10		*Threshold* = 15	
	Mean number of HP packets	Mean number of LP packets	Mean number of HP packets	Mean number LP packets	Mean number of HP packets	Mean number LP packets
0	0	0	0	0	0	0
0.1	0	0.0732	0	0.1216	0	0.2358
0.2	0.0004	0.3413	0	0.7199	0	1.9162
0.3	0.0078	2.0039	0.0001	7.9085	0	27.9068
0.4	0.0884	29.1149	0.0056	36.6219	0.0009	38.5045
0.5	0.6731	38.7473	0.1971	39.413	0.1073	39.7742
0.6	48.7302	39.9841	47.6821	39.9955	47.456	39.9994
0.7	98.2	40	98.2	40	98.2	40
0.8	99.4	40	99.4	40	99.4	40
0.9	99.8	40	99.8	40	99.8	40
1	100	40	100	40	100	40

Table 6
Varying threshold, b changed, leakage 0.01.

Threshold	Mean number of HP packets	Mean number of LP packets
5	48.7302	39.841
10	47.6821	39.9955
15	47.4560	39.9994
20	47.4317	40
25	47.4303	40
30	47.4302	40

Table 7
Varying threshold, a_L changed, leakage 0.01.

Threshold	Mean number of HP packets	Mean number of LP packets
5	48.7302	39.9982
10	47.6821	39.9994
15	47.4560	39.9999
20	47.417	40
25	47.4303	40
30	47.4302	40

number of LP packets in the system, on the other hand, increases slightly, as shown in Tables 6 and 7.

Increasing the threshold of the system results in an increase in the mean number of LP packets in the system and a decrease in the mean number of HP packets in the system.

The model developed as a Geo/Geo/1/k system shows the impact of leakage and threshold on the mean number of LP packets, HP packets and tokens in the system.

6. Conclusion

Motivated by real world implementations of energy harvesting in WSNs in which there is energy leakage, we analysed the energy harvesting sensor node's performance with two assumptions: data transmission and energy leakage occur and the token buffer subjected to a threshold. To study the node, a model with a threshold imposed on the token buffer was developed. We illustrated that the proposed system can be categorised as

a Quasi-Birth–Death process (QBD) which enabled us to determine the performance measures by applying matrix-geometric methods. The simulations revealed the impact of leakage, priority and threshold on the mean number of packets and tokens in the system.

Our findings show models that accurately capture energy usage by the packets and leakage. To ensure that there is always a token available to transmit the HP packet, a threshold is imposed on the energy buffer. However, this approach can lead to loss of LP packets that are also valuable. To overcome this, we propose imposing a delay on the transmission of the LP packets such that after a specified time period the LP packets are transmitted. The model with threshold incorporated is significantly affected by two main factors, the rate of leakage and the threshold. A low rate of leakage results in more tokens being available in the system for transmission of both HP and LP packets. Therefore, the mean number of both HP and LP packets reduces with a reduction in the rate of leakage. A higher threshold will mean that there are more tokens in the system for the transmission of HP packets but less for transmission of LP packets.

CRediT authorship contribution statement

Otim Patricia Angwech: Conception and design of study, Acquisition of data, Analysis and/or interpretation of data, Writing – original draft, Writing – review & editing. **Attahiru S. Alfa:** Conception and design of study, Acquisition of data, Analysis and/or interpretation of data, Writing – review & editing. **B.T.J. Maharaj:** Conception and design of study, Writing – review & editing.

Declaration of competing interest

The authors declare that they have no known competing financial interests or personal relationships that could have appeared to influence the work reported in this paper.

Acknowledgements

We would like to acknowledge SENTECH and the South African Research Chairs Initiative (SARChI) in Advanced Sensor Networks (ASN) for their financial support in making this research possible. Approval of the version of the manuscript to be published.

References

Afsar, M., 2015. Energy-efficient coalition formation in sensor networks: A game-theoretic approach. arXiv preprint arXiv:1512.08019.
Akyildiz, I.F., Su, W., Sankarasubramaniam, Y., Cayirci, E., 2002a. Wireless sensor networks: A survey. Comput. Netw. 38 (4), 393–422.
Akyildiz, I.F., Su, W., Sankarasubramaniam, Y., Cayirci, E., 2002b. A survey on sensor networks. IEEE Commun. Mag. 40 (8), 102–114.
Alfa, A.S., 2010. Queueing Theory For Telecommunications: Discrete Time Modelling Of A Single Node System. Springer Science & Business Media.
Ali, M.S., Singh, R., 2017. A study on game theory approaches for wireless sensor networks. IJEAT ISSN 2249–8958.
Anastasi, G., Conti, M., Di Francesco, M., Passarella, A., 2009. Energy conservation in wireless sensor networks: A survey. Ad Hoc Netw. 7 (3), 537–568.
Angwech, O., Alfa, A.S., Maharaj, B.T., 2020. Analysing usage of harvested energy in wireless sensor networks: A Geo/Geo/1/K approach.. In: SENSORNETS. pp. 71–77.
Ashraf, N., Asif, W., Qureshi, H.K., Lestas, M., 2017. Active energy management for harvesting enabled wireless sensor networks. In: Wireless On-Demand Network Systems And Services (WONS), 2017 13th Annual Conference On. IEEE, pp. 57–60.
Bertsekas, D.P., Gallager, R.G., Humblet, P., 1992. Data Networks, Vol. 2. Prentice-Hall International New Jersey.
Bhat, U.N., 2015. An Introduction To Queueing Theory: Modeling And Analysis In Applications. Birkhäuser.
Charilas, D.E., Panagopoulos, A.D., 2010. A survey on game theory applications in wireless networks. Comput. Netw. 54 (18), 3421–3430.
De Cuypere, E., De Turck, K., Fiems, D., 2018. A queueing model of an energy harvesting sensor node with data buffering. Telecommun. Syst. 67 (2), 281–295.
Dudin, S.A., Lee, M.H., 2016. Analysis of single-server queue with phase-type service and energy harvesting. Math. Probl. Eng. 2016.
Erlang, A.K., 1909. The theory of probabilities and telephone conversations. Nyt. Tidsskr. Mat. Ser. B 20, 33–39.
Gelenbe, E., 2015. Synchronising energy harvesting and data packets in a wireless sensor. Energies 8 (1), 356–369.
Giambene, G., 2014. Queuing Theory And Telecommunications Networks And Applications. Springer Science+ Business Media, Inc.
Gunduz, D., Stamatiou, K., Michelusi, N., Zorzi, M., 2014. Designing intelligent energy harvesting communication systems. IEEE Commun. Mag. 52 (1), 210–216.
Guruacharya, S., Hossain, E., 2018. Self-sustainability of energy harvesting systems: Concept, analysis, and design. IEEE Trans. Green Commun. Netw. 2 (1), 175–192.
Haddad, M., Altman, E., Gaillard, J., Fiems, D., 2012. A semi-dynamic evolutionary power control game. In: International Conference On Research In Networking. Springer, pp. 392–403.
Jeon, J., Ephremides, A., 2015. On the stability of random multiple access with stochastic energy harvesting. IEEE J. Sel. Areas Commun. 33 (3), 571–584.
Jolai, F., Asadzadeh, S., Taghizadeh, M., 2010. A preemptive discrete-time priority buffer system with partial buffer sharing. Appl. Math. Model. 34 (8), 2148–2165.
Jornet, J.M., Akyildiz, I.F., 2012. Joint energy harvesting and communication analysis for perpetual wireless nanosensor networks in the terahertz band. IEEE Trans. Nanotechnol. 11 (3), 570–580.
Kleinrock, L., 1975. Theory. Queueing Syst. 1.
Kong, H.-B., Wang, P., Niyato, D., Cheng, Y., 2017. Modeling and analysis of wireless sensor networks with/without energy harvesting using Ginibre point processes. IEEE Trans. Wirel. Commun. 16 (6), 3700–3713.
Ku, M.-L., Chen, Y., Liu, K.R., 2015. Data-driven stochastic models and policies for energy harvesting sensor communications. IEEE J. Sel. Areas Commun. 33 (8), 1505–1520.
Ku, M.-L., Li, W., Chen, Y., Liu, K.R., 2016. Advances in energy harvesting communications: Past, present, and future challenges. IEEE Commun. Surv. Tutor. 18 (2), 1384–1412.
Lu, X., Wang, P., Niyato, D., Kim, D.I., Han, Z., 2014. Wireless networks with RF energy harvesting: A contemporary survey. IEEE Commun. Surv. Tutor. 17 (2), 757–789.
Ma, Z., Guo, Y., Wang, P., Hou, Y., 2013. The Geo/Geo/1+1 queueing system with negative customers. Math. Probl. Eng. 2013.
Machado, R., Tekinay, S., 2008. A survey of game-theoretic approaches in wireless sensor networks. Comput. Netw. 52 (16), 3047–3061.
Michelusi, N., Badia, L., Carli, R., Corradini, L., Zorzi, M., 2013. Energy management policies for harvesting-based wireless sensor devices with battery degradation. IEEE Trans. Commun. 61 (12), 4934–4947.
Mouapi, A., Hakem, N., Delisle, G.Y., 2017. A new approach to design of RF energy harvesting system to enslave wireless sensor networks. ICT Express.
Niyato, D., Hossain, E., Rashid, M.M., Bhargava, V.K., 2007. Wireless sensor networks with energy harvesting technologies: A game-theoretic approach to optimal energy management. IEEE Wirel. Commun. 14 (4), 90–96.
Ozel, O., Ulukus, S., 2010. Information-theoretic analysis of an energy harvesting communication system. In: 2010 IEEE 21st International Symposium On Personal, Indoor And Mobile Radio Communications Workshops. IEEE, pp. 330–335.
Paradiso, J.A., Starner, T., 2005. Energy scavenging for mobile and wireless electronics. IEEE Pervasive Comput. (1), 18–27.
Patil, K., De Turck, K., Fiems, D., 2018. A two-queue model for optimising the value of information in energy-harvesting sensor networks. Perform. Eval. 119, 27–42.
Patil, K., Fiems, D., 2018. The value of information in energy harvesting sensor networks. Oper. Res. Lett. 46 (3), 362–366.
Shaikh, F.K., Zeadally, S., 2016. Energy harvesting in wireless sensor networks: A comprehensive review. Renew. Sustain. Energy Rev. 55, 1041–1054.
Shi, H.-Y., Wang, W.-L., Kwok, N.-M., Chen, S.-Y., 2012. Game theory for wireless sensor networks: A survey. Sensors 12 (7), 9055–9097.
Sudevalayam, S., Kulkarni, P., 2010. Energy harvesting sensor nodes: Survey and implications. IEEE Commun. Surv. Tutor. 13 (3), 443–461.
Susu, A.E., Acquaviva, A., Atienza, D., De Micheli, G., 2008. Stochastic modeling and analysis for environmentally powered wireless sensor nodes. In: 2008 6th International Symposium On Modeling And Optimization In Mobile, Ad Hoc, And Wireless Networks And Workshops. IEEE, pp. 125–134.
Tadayon, N., Khoshroo, S., Askari, E., Wang, H., Michel, H., 2013. Power management in SMAC-based energy-harvesting wireless sensor networks using queuing analysis. J. Netw. Comput. Appl. 36 (3), 1008–1017.
Tutuncuoglu, K., Yener, A., 2012. Optimum transmission policies for battery limited energy harvesting nodes. IEEE Trans. Wirel. Commun. 11 (3), 1180–1189.

Valentini, R., Dang, N., Levorato, M., Bozorgzadeh, E., 2015. Modeling and control battery aging in energy harvesting systems. In: 2015 IEEE International Conference On Smart Grid Communications. SmartGridComm, IEEE, pp. 515–520.

Vardhan, S., Wilczynski, M., Portie, G., Kaiser, W.J., 2000. Wireless integrated network sensors (WINS): Distributed in situ sensing for mission and flight systems. In: Aerospace Conference Proceedings, 2000 IEEE, Vol. 7. IEEE, pp. 459–463.

Walraevens, J., Fiems, D., Bruneel, H., 2011. Performance analysis of priority queueing systems in discrete time. In: Network Performance Engineering. Springer, pp. 203–232.

Yang, C., Chin, K.-W., 2016. On nodes placement in energy harvesting wireless sensor networks for coverage and connectivity. IEEE Trans. Ind. Inf. 13 (1), 27–36.

Yang, F., Du, L., Chen, W., Li, J., Wang, Y., Wang, D., 2017. Hybrid energy harvesting for condition monitoring sensors in power grids. Energy 118, 435–445.

Yang, J., Ulukus, S., 2011. Optimal packet scheduling in an energy harvesting communication system. IEEE Trans. Commun. 60 (1), 220–230.

Zareei, S., Sedigh, A.H.A., Deng, J.D., Purvis, M., 2017. Buffer management using integrated queueing models for mobile energy harvesting sensors. In: 2017 IEEE 28th Annual International Symposium On Personal, Indoor, And Mobile Radio Communications. PIMRC, IEEE, pp. 1–5.

Zhang, F., Lau, V.K., 2015. Delay-sensitive dynamic resource control for energy harvesting wireless systems with finite energy storage. IEEE Commun. Mag. 53 (8), 106–113.

Zhang, S., Seyedi, A., Sikdar, B., 2013. An analytical approach to the design of energy harvesting wireless sensor nodes. IEEE Trans. Wirel. Commun. 12 (8), 4010–4024.